DESIGN OF A HYBRID RO-MED SOLAR DESALINATION SYSTEM FOR TREATING AGRICULTURAL DRAINAGE WATER IN CALIFORNIA

Authors: ***Adam M. Weiner****, David H. Blum, John H. Lienhard V, Ahmed F. Ghoniem*

Presenter: **Adam Michael Weiner**
Graduate researcher – Massachusetts Institute of Technology – United States
aweiner@mit.edu

Abstract

The current drought in California's Central Valley has placed a significant strain on water supplies for agriculture. Motivated by efforts to renewably expand the water supply through recycling agricultural runoff, we examine the cost benefits of and provide design recommendations for a concentrated solar-powered hybrid reverse osmosis (RO), multi-effect distillation (MED) desalination system for this application. A hybrid RO-MED system operates more efficiently than current standalone MED systems and at recovery ratios beyond the feasibility of current standalone RO systems, reducing energy and disposal costs. Additionally, a concentrated solar power (CSP) source provides both work and heat renewably, without emissions, and allows for remote operation.

We construct a detailed thermodynamic and economic model of the hybrid system and perform a parametric study of the effect of RO operating flux and MED effect number on the levelized cost of water produced. We find that a levelized cost of water reduction of over 41% is possible in employing a hybrid system versus a standalone MED system for a reasonable RO recovery, on the basis of capital and energy requirements, with the savings decreasing at reduced RO recoveries. To minimize the levelized cost of water produced by the hybrid system, we recommend employing five MED effects and operating both RO stages at an average flux of 18.2 LMH. The key tradeoff in identifying the optimal design is between the capital cost of each desalination system and the capital cost of the required concentrated solar power field and power block. We find that the levelized cost of water is most sensitive to the number of effects employed in the MED system. We also develop an economic framework to justify the employment of water storage for the system.

I. INTRODUCTION

1.1 Background

California is currently experiencing its worst drought in recorded history, with nine of its eleven major climate regions recording record-low precipitation for 2013 [1] and the state's mountain snowpack at 20% of the normal amount [2]. The Central Valley Project (CVP) and State Water Project (SWP), federally and state run systems of pumps, reservoirs, and aqueducts, have announced cutbacks on agricultural, urban, and environmental water allocation contracts. The CVP is allocating 0% of agricultural, 50% of municipal and industrial, and 40% of environmental contract amounts [3]. The SWP is allocating 0% of contracts across the board [4].

The impact of the drought is felt state-wide, but perhaps most significantly by the Central Valley Region. California led the nation in agricultural cash receipts in 2012 with $44.7 billion, leads the nation in the production of more than 79 crop and livestock commodities, and accounts for a third of vegetables and nearly two-thirds of fruits and nuts produced in the U.S. [5]. Most of this agricultural output comes from the Central Valley Region. As the drought continues, farmers in the region are fighting to keep their crops irrigated and California's economic backbone intact. Without available surface water, they are turning to the groundwater and drainage water supplies. However, the salinity of the water used must be low to avoid irrigation use restrictions [6] and costly economic impacts [7].

While conjunctive management can help preserve and allocate usable groundwater and agricultural runoff, other methods to extract and reuse inland brackish waters should be explored as dry conditions persist in California, and around the world [8]. Brackish water desalination offers farmers local water access with increased security. The use of on-site renewable energy allows for remote operation and benefits the environment.

This paper proposes and analyzes the design of a solar-powered desalination system for treating the agricultural runoff and brackish waters of California's Central Valley. Specifically, we take advantage of the low energy consumption of a reverse osmosis process, while pushing the recovery ratio beyond RO feasibility with thermal desalination (MED), all while sourcing renewable thermal and electrical energy from concentrated solar power (CSP). Previous research has shown the benefits of membrane-thermal hybridization, including permeate blending, electricity savings from replacing second-stage membrane with thermal systems, and salt production [9, 10], though not in the context of water-power cogeneration. Other research has considered water-power cogeneration through the use of thermal desalination in the condensing portion of conventional Rankine cycles [10-13] or CSP-driven dual purpose plants [14-16]. Additionally, a current implementation uses CSP to power a thermal-only desalination system [17]. This past research however has neither considered the combined benefits of desalination process hybridization and water-power cogeneration with CSP, nor water production as the primary purpose of the plant - which influences storage requirements.

1.2 Research Objectives

This paper proposes and analyzes the design of a renewable hybrid RO-MED desalination system with TVC recovery for the MED process, which is used to increase the process efficiency by recovering enthalpy from the last effect. The system takes advantage of high-efficiency, commercially available RO technology as well as high recovery MED technology. From the perspective of water flows, the RO system takes brackish feed water, desalinates to the limiting recovery ratio, and sends the resulting brine to the MED system, where it is desalinated further. From the perspective of energy flows, the system is powered by a locally-sited CSP plant. The steam produced by the solar collector field runs a Rankine power cycle to produce electricity for the RO system and auxiliary components of the MED system. Turbine exhaust steam drives the MED process. A trough collector solar field collects the solar irradiation, as this method tends to be cheaper than a solar tower on smaller production scales.

The location of the solar desalination system is California's Central Valley Region. The target water supply capacity is 7,600 m^3 of permeate per day, which is currently being pursued commercially in the Valley [17]. The target permeate salinity is 500 ppm, the maximum salinity without use restrictions for irrigation in the Central Valley [6]. The feed salinity is 15,000 ppm, characteristic of local agricultural runoff and local brackish waters, and the recovery ratio of the system is 0.93. Figure 1 below shows an overview of the energy and water flows through the proposed system.

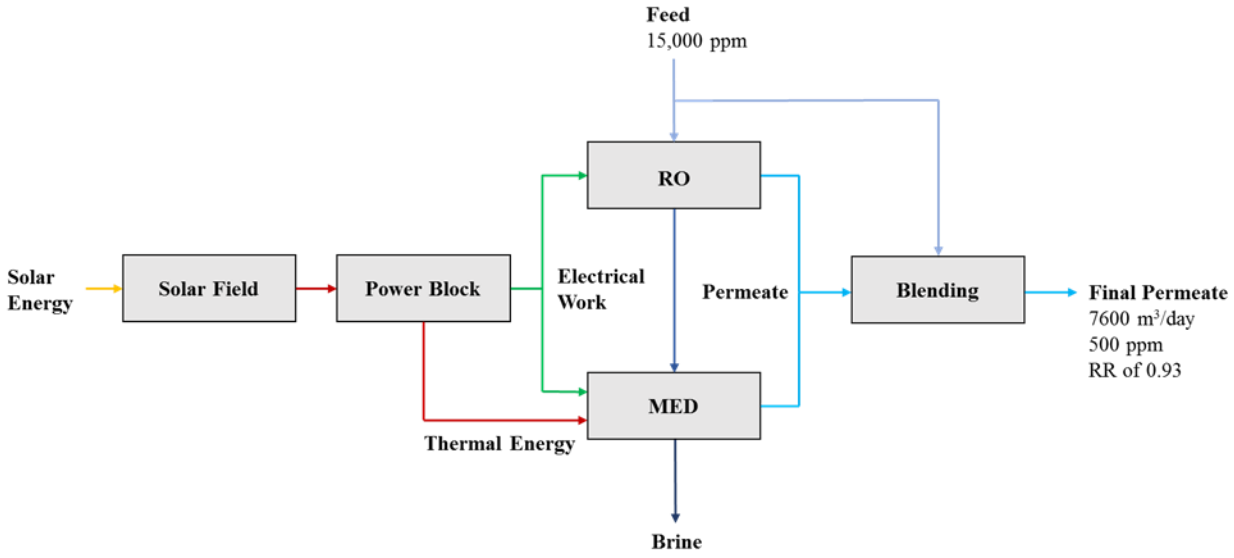

Figure 1 – Energy and water flows through the proposed CSP-powered RO-MED hybrid desalination system

Thermodynamic and economic models of each of the three main system components (RO, MED, and CSP) were constructed in Engineering Equation Solver (EES) [18] and solved numerically. Key design parameters and cost figures are assumed from the literature and compiled in Sect. 2.6. Using this model, parametric analyses of the impact of certain design and operation assumptions on the efficiency and cost of the entire system are conducted. These analyses are also used to optimize the design of the system based on the levelized cost of water ($/$m^3$). Variations of the model are used to compare the proposed hybrid-CSP system with an MED-CSP system as well as to consider the cost premium associated with sourcing energy from the grid instead of a locally-sited CSP plant.

II. MODELLING AND ANALYSIS

2.1 *RO system model*

The purpose of hybridizing the MED-TVC thermal desalination system with reverse osmosis is to significantly reduce the energy consumption of the plant as well the capital costs. On both fronts, reverse osmosis has been shown to significantly outperform thermal desalination technologies. For our application, we propose a two-stage reverse osmosis system with pressure recovery.

The specific energy and capital costs for reverse osmosis are both lower than in MED. Therefore, we maximize RO plant utilization by pushing the system to the highest possible recovery ratio. This maximum recovery ratio may be limited by either feed water fouling potential or the maximum operating pressure of the system. We assume that a prudent pre-treatment process has been designed to reduce the propensity for fouling. Also, the maximum allowable pressure for a typical commercial element is 69 bar [19]. Setting a conservative target, we model the system with an overall recover ratio of 75%. Following industry standards, we set the recovery ratio of both stages equal - each 50%.

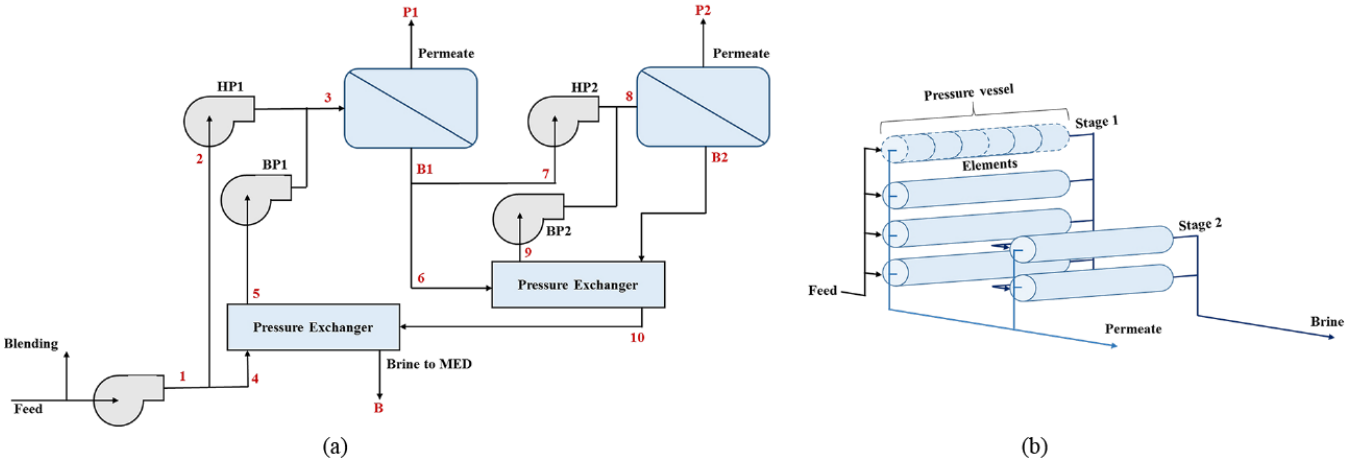

Figure 2 – Components and thermodynamic states of the proposed two-stage RO system with pressure recovery

Figure 2 is a schematic diagram of the RO configuration modeled. Here, we employ two pressure exchangers to recover the high-pressure brine stream emanating from each stage. The feed to the desalination plant is initially split into two streams. 97% of the feed is sent through a low pressure pump, used to overcome hydraulic losses through the circuit. The other 3% is used to blend with the RO and MED permeate streams to ensure a 500 ppm product. Following the low pressure pump, feed moving through the RO system is immediately split into two more streams - one which moves directly to a high pressure pump (HP1), the second to a pressure exchanger for pressure recovery. The pressure of this stream is then raised with a booster pump (BP1) to the required feed pressure (P3) of the first stage. The first stage separates the feed into permeate (P1) and brine (B1). We assume a constant salt rejection of 99.6%. This brine is then split, analogously to the first stage and later recombined to form the feed to the second stage. A second pressure exchanger is employed for the second brine (B2). Two pressure exchangers are required because of a design constraint; the flow rates of two streams passing through a pressure exchanger must be equal. The pressure exchangers are modeled as coupled compressor/turbines with an efficiency, as shown in Equation 1 below [20]:

$$P_5 = P_4 + \eta_r(P_{10} - P_B) \quad (1)$$

where η_r is the efficiency of the pressure recovery system. P_{10} is a free variable in our model set to 30 bar. The desired pressure P_B of the brine exit was set to 2 bar for pumping through the MED-TVC.

The total capital cost of the RO system was determined based on the price per element multiplied by a factor of 3 to account for installation and maintenance costs over the 10-year plant life. The required number of elements n_e for the RO plant is given by Equation 2:

$$n_e = \frac{\dot{q}_{p,RO}}{\Phi A_e} \quad (2)$$

where Φ is the desired average permeate flux, $\dot{q}_{p,RO}$ is the required RO permeate flow rate, and A_e is the active membrane area of an element. To compute the total required membrane area we use the effectiveness-MTU method proposed by Banchik et al. [21].

2.2 *MED system model*

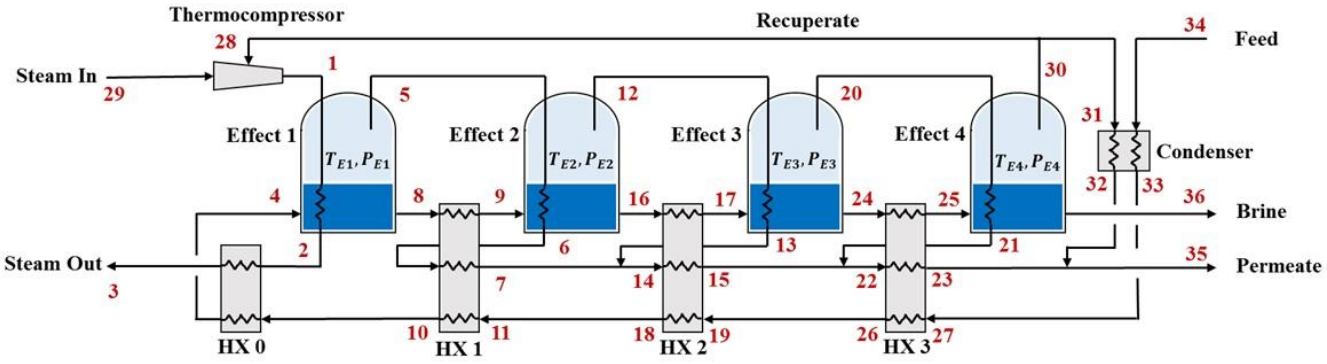

Figure 3 – Components and thermodynamic states of the proposed MED-TVC system

MED systems use multiple distillation chambers (effects) to evaporate and collect pure water from the feed. Figure 3 shows a diagram of the MED system modeled in this study. The diagram shows four effects for illustration; the number of effects is actually optimized to minimize the levelized cost of water (see Sect. 3.2). Each effect is maintained at a different pressure and temperature from the others, corresponding to the saturation condition for water. The temperature is highest at the first effect and steps down at regular intervals through the remaining effects. High temperature steam and feed water enter the first effect and exchange heat such that the high temperature steam condenses and the feed water evaporates. The remaining brine solution is cooled via heat exchange with the incoming feed water and sent to the second effect. The vapor produced by the evaporation process in the first effect is fed into the second effect where it exchanges heat with the cooler brine solution from the first effect. The vapor from the first effect is condensed and the brine in the second effect evaporates. The condensed vapor, or permeate, is cooled via heat exchange with the incoming feed water.
This process is repeated for each of the remaining stages of the system, with the permeate stream being collected at each stage. A portion of the vapor from the last effect is fed to a thermal vapor-compressor (TVC) in which high pressure motive steam is added to increase the temperature and pressure of the resulting mixture to that required by the first effect. Ibrahim [22] cites many advantages of an MED-

TVC system over other thermal desalination systems, including higher gained output ratios (GORs), less effects, lower maintenance costs, lower pumping power, and lower required first-effect temperature.

We set a top temperature of 70℃ and a last effect temperature of 35℃ [23, 24], creating a temperature difference between each effect which depends on the exact number of effects and assuming a linear temperature distribution. Using the above assumptions and given a feed mass flow rate (from the RO system), required permeate mass flow (to make up the difference from the RO system), steam inlet temperature, and number of effects, the required mass flow rate of the CSP plant steam and the outlet condition of the CSP plant steam can be computed. Through successive mass and energy balances around each effect, the required mass flow rate of inlet steam to the first effect $\dot{m}_1$ is given by Equation 3:

$$\dot{m}_1 = \frac{\dot{m}_p}{\sum_i^{N-1} \frac{h_{fg,TE_H}}{h_{fg,TEi}}} \tag{3}$$

where $\dot{m}_p$ is the required mass flow rate of permeate, $h_{fg,TEi}$ is the enthalpy of vaporization for the brine in each effect, and h_{fg,TE_H} is the enthalpy of vaporization for the driving steam. If we assume the MED system does not contain heat recovery through the TVC or condenser, the gained output ratio (GOR) can be defined as in Equation 4 below:

$$\text{GOR} = \frac{\dot{m}_p h_{fg,f}}{Q_{in}} = \frac{\dot{m}_p h_{fg,f}}{\dot{m}_1 h_{fg,1} + \dot{m}_{10}(h_4 - h_3)} \tag{4}$$

Substituting Equation 3 into Equation 4, assuming the change in feed enthalpy is small compared to the condensing of steam and taking all of the enthalpies of vaporization to be similar, reveals that the GOR increases with the number of effects.

2.3 *CSP system model*

The CSP system collects energy from the Sun and converts it into the electrical work required for the RO and MED systems as well as the thermal energy required for the MED system, as shown in Figure 4. Trough collectors are used to collect and concentrate the solar irradiation in order to heat a circulating heat transfer fluid. The fluid exchanges heat with circulating steam in a Rankine cycle power block. High temperature and pressure steam leaves the heat exchanger and enters a high-pressure turbine. A portion of the intermediate pressure steam is then bled off from the turbine in order to feed the MED system. The remainder of the intermediate-pressure steam is reheated by the heat transfer fluid back to a high temperature and fed into a low-pressure turbine. After the low-pressure turbine, the steam is condensed and pumped back up to the intermediate pressure, mixed with liquid water exiting the MED system, as our MED model assumes full condensation of steam through the system, and pumped back up to the high pressure to be heated by the solar field heat exchanger.

Thermal oil (Therminol VP-1) is the chosen as a solar field heat transfer fluid with a specific heat capacity of 1887 J/kg-K and density of 1060 kg/m^3. The solar field operates between temperatures of 295℃ and 390℃ [23]. We assume a collector efficiency, the ratio of heat transferred to the fluid to incident solar irradiation, of 0.55 [25]. For a steady state analysis, the chosen solar irradiation is 500 W/m^2 [20], determined as the average daily (12-hr) irradiation for the Central Valley. For the power cycle, the high-pressure steam is 373℃ [21] and 37 bar. The isentropic efficiency of the turbines is 0.85. We neglect any pump work.

Additionally, we assume the intermediate temperature steam is to be heated back up to 373℃ at the intermediate pressure of 6 bar and that the steam is saturated following the low-pressure turbine at a temperature of 177℃. The condenser outlet is saturated liquid at a pressure of 0.18 bar. From these key assumptions, in addition to the required electrical output to run the RO and MED systems, the other operating states, the required mass flow rate of cycle steam, mass flow rate of thermal oil, and finally, the required solar collector field area may be determined using mass and energy balances around each component and the second law efficiencies of the turbines.

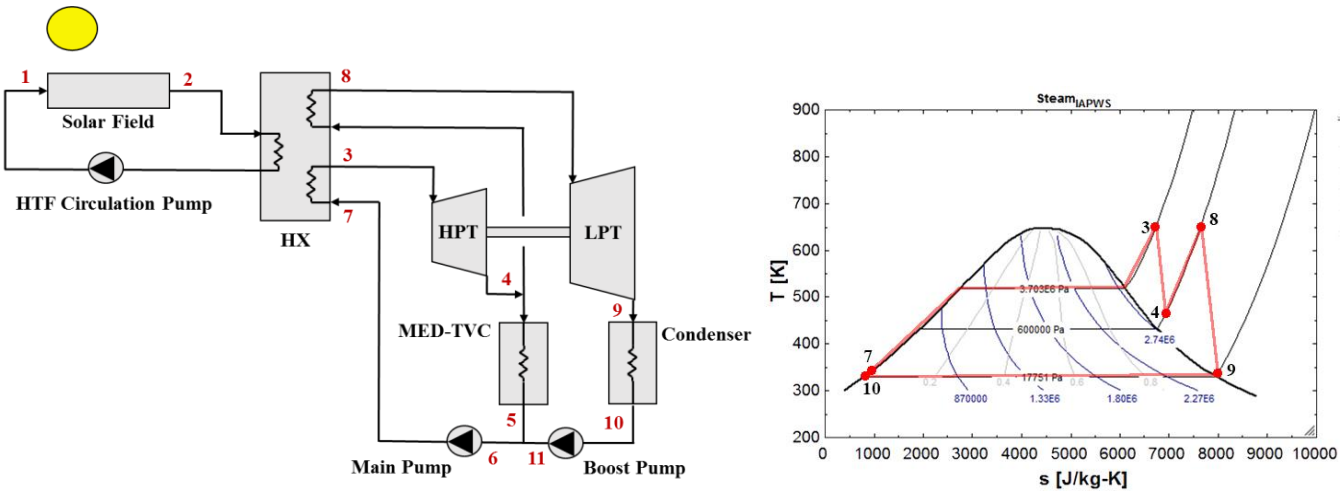

(a) (b)

Figure 4 – Components and thermodynamic states of the proposed CSP system (a) and corresponding T-s diagram (b)

2.4 *Storage system model*

In solar desalination, either water storage or energy storage must be employed to achieve the desired productivity. In water storage, for a capacity factor of 0.5, the desalination system operates at roughly double the desired productivity during the day, storing roughly half of the produced water in tanks, which are then emptied at night. Neither the desalination system nor the CSP plant operate at night. The design implications are that the desalination system must be sized for double the productivity and a water storage system must be installed.

In energy storage, the desalination system consistently runs at the desired productivity, day and night, while the CSP plant only runs during the day. The design implications include desalination plant sizing at the desired productivity as well as energy storage system installation. The CSP plant may also be sized slightly larger than in the water storage plant because of energy storage inefficiencies. In summary, a desalination system employing water storage results in lower CSP capital costs and storage system costs, while the employment of energy storage results in lower desalination system costs.

For a CSP-powered hybrid RO-MED system, we illustrate a possible embodiment of water storage and a possible embodiment of energy storage in Figure 5.

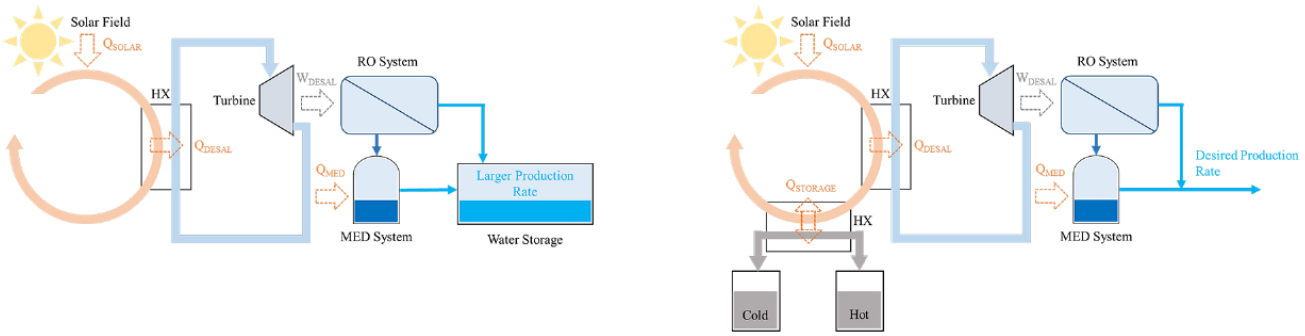

Figure 5 – Operation of a water storage (a) and an energy storage (b) system for a CSP-powered hybrid RO-MED desalination system

For the hybrid system, we optimized the specific cost of water with respect to the reverse osmosis average flux and the number of effects in the MED-TVC for both a water storage and energy storage configuration, assuming a capacity factor ζ of 0.5 and a negligible water storage system cost. The results confirmed our intuition based on the tradeoffs. We calculated a critical energy storage cost of 0.0125 \$/kWh, below which energy storage is cost advantageous to water storage. As current energy storage technologies are orders of magnitude more expensive, we conclude that employing water storage is cost advantageous. Our analysis proceeds assuming water storage is employed, with a capacity factor of 0.5.

2.5 *Hybrid system cost model*

The contribution to the levelized cost of water for the hybrid system consists of specific capital costs (in \$/m^3) for the CSP plant, RO system, and MED-TVC system. The capital cost modeling method and formulas are listed below.

- Specific capital cost of the CSP plant, Ξ_{CSP}

$$\Xi_{CSP} = \frac{(\mathrm{K_{pb}}+\mathrm{K}_{op})\dot{\mathrm{W}}_{\mathrm{CSP}}+(\mathrm{K_C}+\mathrm{K_L})\mathrm{A_C}}{\dot{\mathrm{q}}_{\mathrm{p,tot}}\mathrm{CAF}} \quad (5)$$

where $\mathrm{K_{pb}}$ is the power block cost (in \$/kW), K_{op} is the operation and maintenance cost (in \$/kW), $\dot{\mathrm{W}}_{\mathrm{CSP}}$ is the total power output of the CSP plant (in kW), $\mathrm{K_C}$ is the collector cost per area (in \$/m^2), $\mathrm{K_L}$ is the land cost (in \$/m^2), $\mathrm{A_C}$ is the collector area (in m^2), $\dot{\mathrm{q}}_{\mathrm{p,tot}}$ is the total production rate (in m^3/day), and CAF is the capital amortization factor (in days):

$$\mathrm{CAF} = \frac{1}{r}\left[1-\left(\frac{1}{1+r}\right)^{\tau}\right] \quad (6)$$

where r is the annualized cost of capital (10%) and τ is the lifetime of the plant (10 years).

- Specific capital cost of the RO plant, Ξ_{RO}

$$\Xi_{RO} = \frac{\mathrm{K}_{RO}(n_{e,1}+n_{e,2})}{\dot{\mathrm{q}}_{\mathrm{p,tot}}\mathrm{CAF}} \quad (7)$$

where K_{RO} is the cost per element (in $) and $n_{e,1}$ and $n_{e,2}$ are the number of elements in the first and second stages

- Specific capital cost of the MED-TVC plant, Ξ_{MED}

$$\Xi_{MED} = \frac{K_N N}{\dot{q}_{p,tot} CAF} \quad (8)$$

where K_N is the cost per effect (in $) and N is the total number of effects.

2.6 *Key model parameters*

Important model parameters are compiled in Table 2 below. To the extent possible, values of the parameters were tailored to local data reported in the Central Valley.

Table 2 – Key cost and system parameters implemented in the model

Symbol	Description	Value	Ref.
RO System Parameters			
A_e	active area	35 m^2	[19]
η_r	press. recovery eff.	0.96	[20]
K_{RO}	cost/element	$700	[19]
L_w	water permeability	1.1 L/m^2-hr-bar	[19]
ξ	salt rejection	0.996	[19]
MED System Parameters			
K_N	cost/effect	$0.9M	[24]
$T_{e,i}$	first effect temp	70°C	[23, 24]
$T_{e,f}$	last effect temp	35°C	[23, 24]
W_{MED}	auxiliary work	1.2 kWh/m^3	[27]
CSP System Parameters			
η_C	collector efficiency	55%	[25]
I_s	solar irradiation	500 W/m^2	[26]
K_C	collector cost	330 $/$m^2$	[28]
K_L	land cost	10,000 $/acre	[28]
K_{op}	operation cost	650 $/kW	[28]
K_{pb}	power block cost	940 $/kW	[28]
General System Parameters			
K_e	electricity price	0.07 $/kWh	[29]
K_g	gas price	0.014 $/kWh	[30]
$\dot{q}_f$	production rate	7600 m^3/day	[17]

RR_{sys}	system recovery	0.93	[17]
S_f	feed salinity	15,000 ppm	[17]
$S_{p,f}$	product salinity	500 ppm	[6]

III. RESULTS

3.1 *RO system design recommendations*

In determining the membrane area, there is a tradeoff between capital and energy costs with respect to the average operating flux Φ. As the membrane area decreases and the flux increases, the capital cost of the plant decreases but at the expense of greater energy consumption. To illustrate the tradeoff, we model the specific cost of water produced by the RO system alone, powered by electricity from the grid, and we plot the specific energy and capital cost contributions versus the operating flux in Fig. 6 (a). The optimal average flux is 21.3 LMH.

The total specific cost of water produced by the hybrid system versus the RO flux is plotted in Fig. 6 (b). The capital cost contributions from the CSP plant, MED system, and RO system are also plotted. The number of MED effects is fixed at five. Here, the CSP capital cost (effectively the specific energy cost) and the RO capital cost trade off; the MED specific capital cost remains constant. The optimal RO operating flux (18.2 LMH) is smaller than in Fig. 6 (a) because, in employing the CSP plant, the specific cost of energy relative to the specific cost of capital is greater.

Additionally, we observe that the specific cost of water produced by the hybrid system varies only mildly with RO flux. This is because the capital cost of the RO system represents a very small percentage of the total system capital cost. Consequently, a simple optimization procedure in which the optimal RO operating flux is determined followed by the optimal number of MED effects is justified.

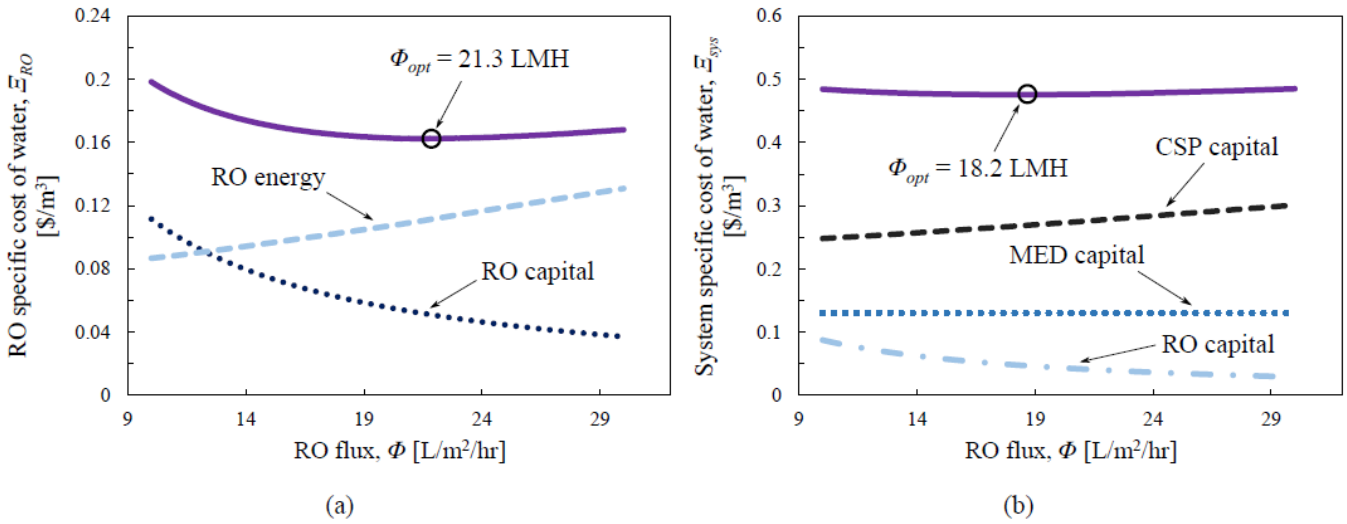

Figure 6 – Energy and capital requirements versus RO operating flux for the isolated RO system powered by the grid (a) and the RO system in the hybrid configuration (b)

3.2 *MED system design recommendations*

A similar tradeoff between energy consumption and capital cost is found in determining the optimal number of effects for the MED system. Figure 7 (a) illustrates the tradeoff between CSP capital and MED capital for an MED-only system employed in the same application and sourcing thermal energy from a CSP plant complemented by grid electricity for the auxiliaries. The optimal number of effects is 13. The relatively large number of effects reflects the high electricity price and importance of high thermal efficiency, a result of employing CSP. Figure 7 (b) shows the specific cost of water and the cost contributions for the complete hybrid system, varying only the number of MED effects. The optimal number of effects is 5. Fewer effects are optimal in the hybrid case, because the overall energy efficiency of the process is higher; the CSP capital cost relative to the MED capital cost is much lower. The specific cost of water is much lower for the hybrid system, because the CSP capital costs are reduced. We also observe, in the hybrid configuration, significant specific cost increases in deviating from the optimum, as the MED capital and energy requirements dominate the total specific cost of water produced.

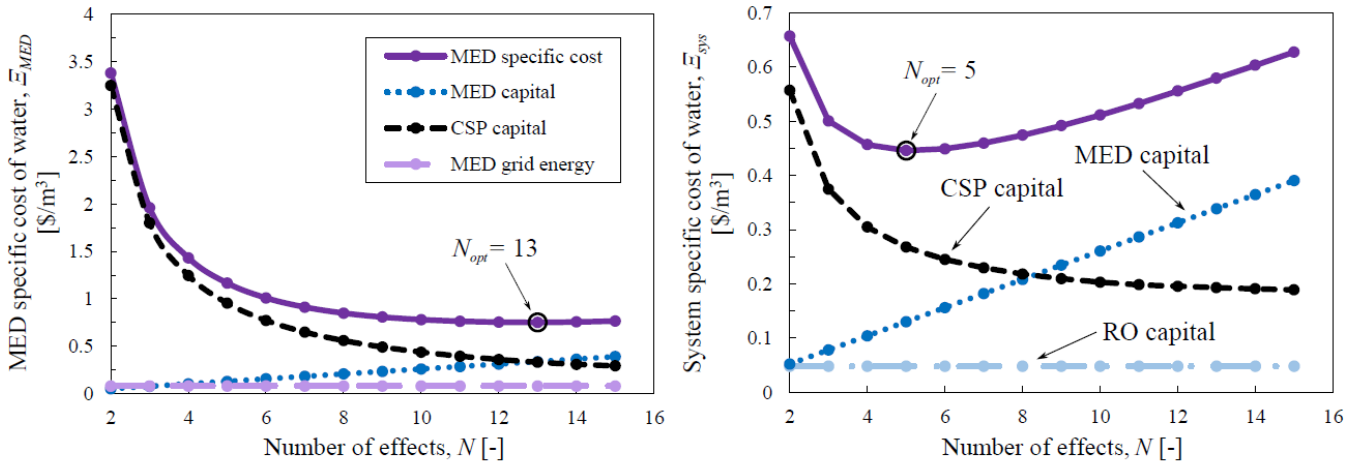

Figure 7 – Energy and capital requirements versus number of MED effects for the MED-only system (a) and for the hybrid configuration (b)

3.3 *Performance and cost comparison with a standalone MED system*

A comparison of the levelized cost of water produced in the proposed hybrid RO-MED system to a stand-alone MED system reveals significant cost savings. For the MED-only system, thermal energy is sourced from the CSP plant and electricity for pumping, controls, etc. is sourced from the grid. Figure 8 (a) shows a levelized cost of water which is 41% lower when produced by the hybrid system. When the hybrid system is powered by natural gas and grid electricity, the levelized cost of water is 48% lower. Overall, most of the cost savings are attributed to the improved energy efficiency of the hybrid configuration. Additionally, the hybrid system with CSP is cost competitive with the hybrid system powered by natural gas and grid electricity, because water storage is employed.

The water produced by each CSP-powered desalination solution costs less than what is currently available for Central Valley farmers (0.81-1.62 $/m^3 [31]). We estimate a specific cost of water for the hybrid configuration with CSP to be 0.45 $/m^3 with an initial capital investment of $13.8M. We estimate a specific cost of water for the MED-only system to be 0.75 $/m^3 with an initial capital investment of $23.2M.

In both hybrid systems modeled in Figure 8 (a), the overall recovery ratio of the RO system is 0.75. If, however, fouling and/or pressure considerations limit the operation of the RO system to a lower recovery ratio, the savings will be reduced. Figure 8 (b) shows the expected savings across a range of RO system recovery ratios. Even for a total RO recovery of 0.1, the projected cost savings are over 12%. Savings increase with higher RO recovery ratios primarily because of reduced energy consumption resulting in smaller CSP capital costs; the capital cost of the RO-MED desalination system across all RO recoveries is approximately constant.

Figure 8 (b) provides guidance on deciding between an MED-only and a hybrid desalination system design for treating agricultural drainage water in the Central Valley. Provided the additional pretreatment costs associated with operating the RO system at a specific recovery are less than the projected savings, the hybrid system is cost advantageous. To analyze this further, an examination of RO pretreatment requirements for the agricultural drainage water at various recovery ratios is recommended as the subject of future research.

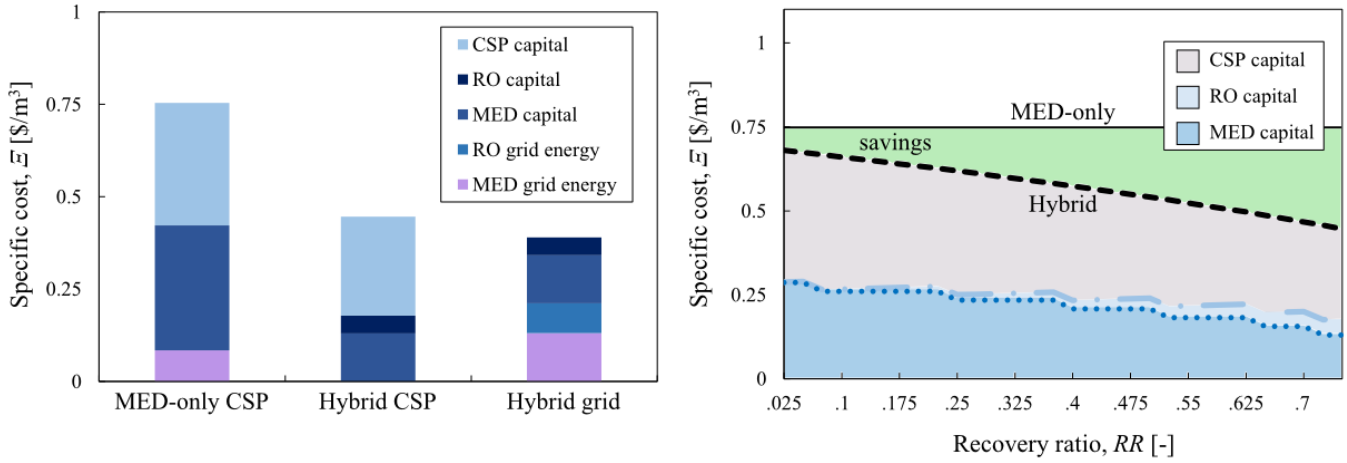

Figure 8 – The projected savings in the levelized cost of water realized by the hybrid RO-MED system for an RO system recovery ratio of 75% (a) and across a wide range of RO recoveries (b)

IV. CONCLUSIONS

On the basis of energy and capital, a concentrated solar-powered hybrid RO/MED plant provides significant cost benefits over a concentrated solar-powered standalone MED system for treating agricultural runoff in the Central Valley. Currently, both desalination solutions offer savings to Central Valley farmers. Additionally, the cost premium associated with employing concentrated solar power over grid energy is partially mitigated through the implementation of water storage. Given the hybrid RO-MED system compares favorably to the standalone MED system, a study of the performance of a pilot plant under field conditions is warranted. Such a study could be devoted to understanding the impact of system fouling and scaling on pretreatment costs as well as the system response to variations in feed water salinity.

VI. REFERENCES

1. California Department of Water Resources. DWR Drops State Water Project Allocation to Zero, Seeks to Preserve Remaining Supplies. 2014. (Accessed March, 2014).
2. The Associated Press. California farmers told not to expect U.S. water. http://www.nytimes.com, 2014. (Accessed March, 2014).
3. Bureau of Reclamation. “Reclamation announces initial 2014 Central Valley project water supply allocation.” http://www.usbr.gov/newsroom, 2014. U.S. Department of the Interior
4. C. A. Torgersen. Notice to State Water Project Contractors. Department of Water Resources, 2014. (Accessed March, 2014).
5. USDA. California Agricultural Statistics 2012 Crop Year. National Agricultural Statistics Service, 2013.
6. Davis, G., M. D. Nichols, and M. J. Spear. California's Groundwater Bulletin 118 Update 2003, Chapter 6. California Department of Water Resources, 2003.
7. Howitt, R. E., J. Kaplan, D. Larson, D. MacEwan, J. Medellin, G. Horner, and N. S. Lee. The Economic Impacts of Central Valley Salinity. University of California Davis, 2009.

8. A. Dai. Increasing drought under global warming in observations and models. Nature Climate Change, 3(1):52-58, August 2012.
9. Turek, M. (2002). "Seawater desalination and salt production in a hybrid membrane-thermal process." *Desalination*, 153, 173-177.
10. Zak, G. M., A. Ghobeity, M. H. Sharqawy, and A. Mitsos (2013). "A review of hybrid desalination systems for co-production of power and water: analyses, methods, and considerations. *Desalination and Water Treatment*, 51:28-30, 5381-5401.
11. Kronenberg, G. and F. Lokiec (2001). "Low-temperature distillation processes in single- and dual-purpose plants." *Desalination*, 136, 189-197.
12. I. Kamal (2005). "Integration of seawater desalination with power generation." *Desalination*, 180, 217-229.
13. Yang, L. and S. Shen (2007). "Assessment of energy requirement for water production at dual-purpose plants in China." *Desalination*, 205, 214-223.
14. Trieb, F. and H. Muller-Steinhagen (2008). "Concentrating solar power for seawater desalination in the Middle East and North Africa." *Desalination*, 220, 165-183.
15. Moser, M., F. Trieb, and J. Kern (2010). "Combined water and electricity production on industrial scale in the MENA countries with concentrating solar power." German Aerospace Center (DLR), Study for the German Ministry of Environment, Nature Conservation and Nuclear Safety, Stuttgart.
16. Olwig, R., T. Hirsch, C. Sattler, H. Glade, L. Schmeken, S. Will, A. Ghermandi, and R. Messalem (2012). "Techno-economic analysis of combined concentrating solar power and desalination plant configurations in Israel and Jordan." *Desalination and Water Treatment*, 41:1-3, 9-25.
17. WaterFX. http://waterfx.co/. (Accessed October, 2014).
18. Klein, S., F. Alvarado, Engineering Equation Solver, F-Chart Software (2014).
19. Dow Water & Process Solutions. FilmTec SW30HR-380 High Rejection Seawater RO Element. The Dow Chemical Company, 2030 Dow Center Midland, MI 48674.
20. Thiel, G. P., E.W. Tow, L.D. Banchik, H.W. Chung, and J. H. Lienhard V (2015). "Energy consumption in desalinating produced water from shale oil and gas extraction." *Desalination*.
21. Banchik, L. D., M. H. Sharqawy, and J. H. Lienhard V (2014). "Effectiveness-mass transfer units (ε-MTU) model of a reverse osmosis membrane mass exchanger." *Journal of Membrane Science* 458: 189-198.
22. Al-Mutaz, I. S., and I. Wazeer. "Current status and future directions of MED-TVC desalination technology." *Desalination and Water Treatment* ahead-of-print (2014): 1-9.
23. Lienhard V, J. H., M. A. Antar, A. Bilton, J. Blanco, and G. Zaragoza. Solar desalination. Annual Review of Heat Transfer, 15:277-347, 2012.
24. IAEA. Desalination economic evaluation program (DEEP), 2013. http://www.iaea.org/NuclearPower/Desalination/. (Accessed May, 2014).
25. J. Karni (2012). "Solar-thermal power generation." *Annual Review of Heat Transfer*, 15:37-92.
26. National Renewable Energy Laboratory. NREL Prospector. http://maps.nrel.gov/prospector, 2014. (Accessed March, 2014).
27. A. Ophir and F. Lokiec (2013). "Review of MED Fundamentals and Costing." IDE Technologies, Ltd.
28. National Renewable Energy Laboratory. System advisor model (SAM), 2010. https://sam.nrel.gov/.
29. US Energy Information Administration. Electric Power Monthly. http://www.eia.gov/electricity/monthly. (Accessed January, 2015).
30. US Energy Information Administration. Natural gas citygate price in California, 2014. http://www.eia.gov. (Accessed May, 2014).
31. Vekshin, A. California water prices soar for farmers as drought grows. http://www.bloomberg.com, 2014. (Accessed February, 2015).

VII. ACKNOWLEDGEMENT

The authors acknowledge Ronan McGovern and Leonardo Banchik for their guidance and insight in support of this study. Adam Weiner acknowledges support from the Keck Travel Award in Thermal Sciences from the MIT Department of Mechanical Engineering.